Anal. Chem.**2005,** 77,955-963

Articles

Quantitative Predictions to Conditions of Zwitterionic Stacking by Transient Moving Chemical Reaction Boundary Created with Weak Electrolyte Buffers in Capillary Electrophoresis

Cheng-Xi Cao,*,†,‡ Wei Zhang,† Wei-Hua Qin,† Shan Li,† Wei Zhu,† and Wei Liu‡

Laboratory of Analytical Biochemistry & Bioseparation, School of Life Science and Biotechnology, Shanghai Jiao Tong University, Shanghai 200240, China, and Department of Chemistry, University of Science and Technology of China, Hefei 230026, China

This paper develops a novel procedure of quantitativepredictions for the on-column stacking conditions of a zwitterionic analyte by a moving chemical reaction boundary (MCRB) in capillary electrophoresis (CE). The procedure concerns the choice of the weak acidic running and alkaline sample buffers and the velocity design of MCRB created with the two buffers. Based on the theory of MCRB, the theoretical computations are performed.From the computations, the following two predictions are refined for the stacking onditions of zwitterion. (1) The zwitterion velocity in the acidic buffer should be greater than that of MCRB moving toward the cathode, or the zwitterion cannot be well stacked by the MCRB. (2) The gap between pH values of the acidic and alkaline sample buffers ought to comprise the isoelectric point (p*I*) of zwitterion to be stacked; namely. there exists the relation of pH (acidic buffer) < p*I* < pH (sample). The predictions are quantitatively proved by the experiments of zwitterionic stacking with two kinds of MCRBs. In addition, the experiments also show the tightly stacked peak of zwitterion existing in the process of MCRB, but not after the MCRB. The theoretical and experimental results hold obvious significances to other zwitterion (such as peptide and protein) on-column stacking in CE.

On-column stacking, viz., preconcentration, of analytes in a sample matrix has become a simple, convenient, and economical but very powerful tool used to greatly improve the detection sensitivity of capillary electrophoresis (CE). In 1988-1992, Boc˘ek et al.[1,2] developed the preconcentration of transient isotachophoresis (tITP) in CE and Jandik and Jones[3] achieved over 100-fold sensitivity increase by tITP. Almost at the same time, Chien and Burgi[4-8] created the field amplification sample injection (FASI) and really concentrated analytes up to 1000-fold in CE. In 1998, Quirino and Terabe[9] successfully enhanced the sensitivity of micellar electrokinetic chromatography over 5000-fold. Recently, Yang et al.[10] enhanced the sensitivity of CE 7000-fold with FASI coupled with nonuniform electrical field, and Zhang et al.[11]decreased the detection limit of CE greater than 10 000-fold with a pure FASI technique. Significantly, Quirino and Terabe[12] improved the sensitivity of CE up to a millionfold with FASI joined with sweeping method.Importantly, numerous methods of preconcentration for analytes were successfully developed during the past decade. The tITP[1,2,12] and FASI [4-8,10,11] that were developed during the early stage of 1990s were mentioned above. The following will further supply a few of notable cases. From 1998 to 2002, Quirino et al.[9,13-15] and Palmer et al.[16-18] pictured a novel sweeping procedure for the stacking of neutral and charged analytes by the interaction between micellar molecular and analytes. During the period 2000-2003, Britz-McKibbin, Chen et al.[19-21] invented the pH junction stacking for the reconcentration of analytes in a sample matrix. In 1996-2003, Lunte's group[22-25] advanced the pHmediated stacking method for analyses of drugs in a biological sample matrix. In 2002, Shihabi[26,27] added many kinds of watermiscible organic solvents (such as acetonitrile, acetone, and alcohols) into salt sample matrixes. The water-miscible organic solvents can induce a FASI mechanism by decreasing the ionization of salt in the sample matrix, can provide the high electric field strength necessary for band sharpening, and consequently can lead to ionizable analyte concentration in sample matrixes even with some salt.

In 2002, we[28,29] developed the stacking procedure of moving chemical reaction boundary (MCRB) for the enhancement of separation efficiency of CE and realized higher than 200-fold improvement of detection sensitivity of analyte in the sample matrix with high salt. Recently, our group achieved up to 3 millionfold enhancement of detection sensitivity and simultaneous separation of zwitterions induced by a single MCRB in CE.[30] All of these experimental studies on sample stacking[28-30] were based on the concept of MCRB[31,32] and its relative method[33-35] developed from 1997 to 2002. However, the relative theoretical studies on the stacking of zwitterionic analytes by the MCRB method have not been carried out up to now. In addition, there are still, to authors' knowledge, no investigations of quantitative theoretical design on conditions of sample stacking in CE.

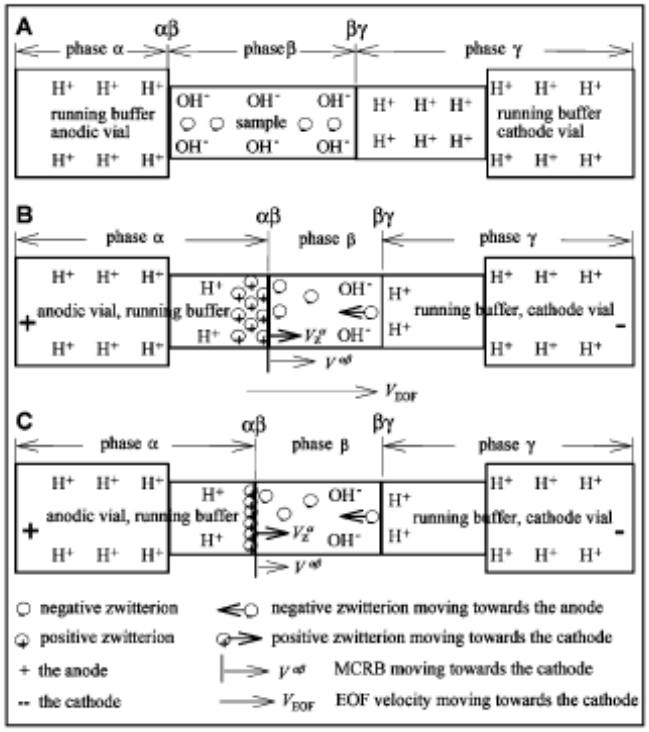

Figure 1. Mechanism of poor or good zwitterion stacking by MCRB moving toward the cathode. (A) The initial state of stacking after injection of weak alkaline sample; (B) the formation of the MCRB after use of electric field, the fast movement of the MCRB toward the cathode, and the poor stacking of zwitterion by the MCRB due to $V_{R\hat{a}} > V_{z\,R}$; (C) the formation of the MCRB after use of electric field, the slow movement of the MCRB toward the cathode, and the good stacking of zwitterion by the MCRB due to $V_{R\hat{a}} \approx V_{zR}$.

Therefore, the main purposes in the paper are to first apply the theory of MCRB[31,32] for accurate predictions to the experimental conditions of MCRB stacking and quantitative illumination on the mechanism of MCRB stacking of zwitterion. These studies are an important step to the quantitative design of zwitterion stacking by the MCRB. Furthermore, we observe the tightly stacked peak of zwitterion existing during the process of MCRB but not after the MCRB. Here, we describe the theoretical and experimental procedure and report the relative results. The MCRB-induced 3 millionfold enhancement of detection sensitivity of zwitterions in CE will be presented in ref 30.

THEORY AND CALCULATION

Phase. A phase is a homogeneous solution demarcated by a moving or stationary boundary. In Figure 1A, there are phases R, *â*, and *ç*, which are in correspondence with the acidic running buffer holding H^+, the alkaline sample matrix containing OH^-, and the running buffer, respectively. Phases R and *ç* are the same running buffer, but they have different functions. The MCRB in Figure 1A is created between phases R and *â* but not between phases *â* and *ç*. Thus, phase R is used for the formation of MCRB, whereas phase *ç* is used for the separation of analytes after the end of MCRB stacking (for the details, see Figure 7 in ref 29).

Expression of MCRB. Using an expression similar to that used for a moving boundary system by MacInnes and Longs-worth,[36-40] the MCRB system in Figure 1A can be briefly expressed as

$$\text{acidic buffer } (+, \alpha) \,||\, \text{alkali } (-, \beta)$$

where, jj implies a boundary being stationary or moving toward the anode or cathode, + and - indicate the anode and cathode, respectively, and R and *â* mean phases R and *â*, respectively. With the basic expressing mode, one can well write the two MCRB systems used here, as will be shown in boundaries 1 and 2 below.

Velocity of MCRB. As shown in Figure 1, the MCRB is created between phases R and *â*, when the electric field is applied. The boundary velocity can be computed with the following equations as have been shown in refs 31 and 32,

$$V^{\alpha\beta} = \left(\frac{m^{\alpha}_{H^+} c^{\alpha}_{H^+}}{\kappa^{\alpha}} - \frac{m^{\beta}_{OH^-} c^{\beta}_{OH^-}}{\kappa^{\beta}}\right) \frac{i}{c^{\alpha}_{H^+} - c^{\beta}_{OH^-}} \qquad (1)$$

$$V^{\alpha\beta} = \left(\frac{m^{\alpha}_{H^+} \bar{c}^{\alpha}_{H^+}}{\kappa^{\alpha}} - \frac{m^{\beta}_{OH^-} \bar{c}^{\beta}_{OH^-}}{\kappa^{\beta}}\right) \frac{i}{\bar{c}^{\alpha}_{H^+} - \bar{c}^{\beta}_{OH^-}} \qquad (2)$$

where c is the equivalent concentration (equiv m^{-3}). The bar over c means the constituent concentration; it does not apply to an ion but to the equilibrium mixture of all subspecies of a constituent (see eqs 4 and 5). The subscripts H^+ and OH^- indicate the hydrogen and hdyroxyl ions, respectively, and the superscripts R and *â* imply phases R and *â*, respectively. The signed quantity is positive if the ion carries net positive charge(s) and negative if net negative charge(s), as has been treated by numerous scientists.[31-40] i is the electric current intensity (A m^{-2}) in capillary. m is the mobility (m^2 V^{-1} s^{-1}). The bar over m indicates the constituent mobility (see eq 3 and 4). Other symbols are the same as those for c. $V_{R\hat{a}}$ is the velocity (m s^{-1}) of MCRB, and _ is the specific conductivity of electrolyte in a phase (S m^{-1}).Equation 1 holds validity for a MCRB created with system of strong electrolytes,[31,32] e.g., HCl (+, R) jj NaOH (-, *â*), while eq 2 is valid to the system of pure weak electrolytes,[31-35] such as CH_3COOH (+, R) jj NH_3H_2O (-, *â*). In eq 2, the constituent mobility and concentration are respectively defined as

$$\bar{m} = \sum a_i m_i \qquad (3)$$

$$\bar{c} = \sum c_i \qquad (4)$$

where m_i is the mobility of subspecies i and a_i is the fraction of subspecies i with mobility m_i, viz.,

$$a_i = c_i/\bar{c} = c_i/\sum c_i \qquad (5)$$

General Conditions of Stacking Zwitterion by MCRB. For convenience of computation, amino acid is used as the zwitterion example for the theoretical investigation of stacking. In the electrolyte arrangement of Figure 1, the pH values of phases R and *â*, which can produce the stacking effect to a zwitterion, are in accordance with the following inequality

$$\mathrm{pH}^{\alpha} < \mathrm{p}I < \mathrm{pH}^{\beta} \qquad (6)$$

For near-maximum stacking of amino acid, inequality 6 shouldbe reexpressed as the much better conditional inequality below

$$\mathrm{pH}^{\alpha} + 2 \le \mathrm{p}K_1 < \mathrm{p}I < \mathrm{p}K_2 \le \mathrm{pH}^{\beta} - 2 \qquad (7)$$

Over 99% of the zwitterion carries a negative charge if it is in phase *â* or a positive charge if it is in phase R under the conditions of expression 7. In inequality 7, pK_1 and pK_2 are the negative logarithms of dissociation on carboxyl and amino groups of amino acids, respectively. But for these amino acids of Lys, Arg, and His,[41] inequality 7 should be expressed as

$$\mathrm{pH}^{\alpha} + 2 \le \mathrm{p}K_R < \mathrm{p}I < \mathrm{p}K_2 \le \mathrm{pH}^{\beta} - 2 \qquad (8)$$

because these three kinds of amino acids have an ionizable side group. In inequality 8, pK_R is the negative logarithm of dissociation on the side chain of an amino acid. In some cases (for example, the pK_1 and pK_2 of isoleucine are 2.36 and 9.69, respectively[41]), there is $pK_2 - pK_1 > 7$; hence, under this condition, inequality 7 and 8 are changed to

$$\mathrm{pH}^{\alpha} \le \mathrm{pH}^{\beta} - 11 \qquad (9)$$

Inequality 9 means a huge gap between pH_R and $pH_{\hat{a}}$ values.Therefore, if the design of pH_R and $pH_{\hat{a}}$ in accordance with inequalities 7-9 cannot be easily realized, one can use inequalities 10 and 11 to design the electrolytic system of MCRB for stacking

$$\mathrm{pH}^{\alpha} \le \mathrm{p}K_1 < \mathrm{p}I < \mathrm{p}K_2 \le \mathrm{pH}^{\beta} \qquad (10)$$

$$\mathrm{pH}^{\alpha} \le \mathrm{p}K_R < \mathrm{p}I < \mathrm{p}K_2 \le \mathrm{pH}^{\beta} \qquad (11)$$

which imply that at least 50% zwitterion carries a positive charge if it is in phase R or a negative charge if it is in phase *â*. Inequality 11 is formulated for the these amino acids Lys, Arg, and His.[41]

Stacking Condition of Zwitterion by MCRB Created with Weak Electrolyte Buffer. For convenience, the following assumptions are given briefly. (1) The absolute mobility of a monovalence negative amino acid is considered to be approximately equal to that of the positive amino acid, as has been shown by Svensson.[42,43] This treatment will be used for the computation of amino acid mobility as shown in Table 1.

Table 1. Basic Physical Chemical Parameters of L-Tryptophan[a]

property	pK_1	pK_2	pI	MW	mobility[b] ($m^2 s^{-1} V^{-1}$)
data	2.83	9.13	5.48	165	1.79×10^{-8}

[a] The data are cited from ref 41. [b] The mobility of monovalent charge Trp calculated from detected data in Figure 4A.

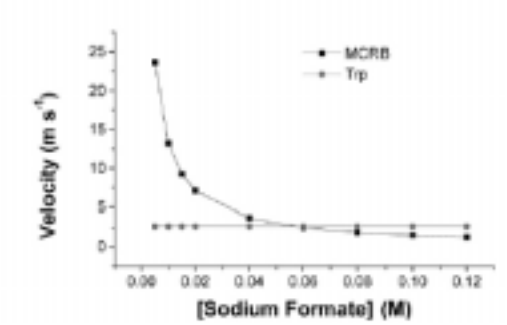

Figure 2. Comparisons between Trp and MCRB velocities in the system of boundary 1. The boundary velocities are computed with eqs 15 and 16 and Trp velocity with eqs 3 and 13. Conditions: i) 2265 A/m2 (set in accordance with the runs in Figure 5); _ values of sodium formate solutions are given in Table 2, as well as the Supporting Information.

(2) The boundaries investigated here are designed to migrate toward the cathode. Figure 1A shows that initial state after the injection of weak alkaline sample matrix. Figure 1B shows that if the velocity of the boundary toward the cathode is over that of the zwitterion in phase R, there exist the following expressions,

$$V^{\alpha\beta} > V_z^{\alpha} \qquad (12)$$

$$V_z^{\alpha} = m_z^{\alpha} E^{\alpha} \qquad (13)$$

the positive zwitterion in phase R near the MCRB cannot catch up with the boundary moving toward the cathode so can be partially, even poorly, stacked. The larger the difference of $V_{R\hat{a}} - V_{z\,R}$ is, the poorer the stacking of the zwitterion by the MCRB. These analyses will be indicated by the predictions of Figures 2 and 3 and proved by the experiments of Figures 5, 7, and 8 as well as Figures S1 and S2 (Supporting Information). In eqs 12 and 13, $V_{z\,R}$ is the velocity (m s^{-1}) of the zwitterion in phase R. $mj_{z\,R}$ is the constituent mobility (m^2 V^{-1} s^{-1}) of the zwitterion in phase R which can be detected with a CZE as shown in Figure 4A.

To well stack the sample plug injected, evidently the velocity of MCRB must fit to the following expression

$$0 < V^{\alpha\beta} \leq V_z^{\alpha} E^{\alpha} \qquad (14)$$

Under the condition of expression 14, good stacking of analyte can be achieved as shown in Figure 1C. The meanings of expression 14 will be shown in Figures 2 and 3 and proved by the experiments of Trp stacking by the numerous MCRBs in Figures 5-8 and S1-S5 (Supporting Information).

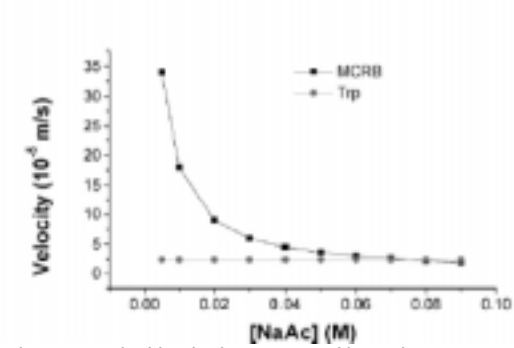

Figure 3. Comparisons of Trp and MCRB velocities in the system of boundary 2. MCRB velocities are computed with eqs 15 and 16 and Trp velocity with eqs 3 and 13. Conditions: i) 4530 A/m2; _ values of phase *â* are given in Table 3, as well as the Supporting Information.

As proved in the papers,[33-35] eq 2 should be given as eq 15 under the conditions of MCRB moving toward the cathode and of weak acidic buffer in phase R due to the background salts (sodium formate in the formic buffer of boundary 1 and sodium acetate in the acetic buffer of boundary 2 shown below).

$$V^{\alpha\beta} = \left(\frac{\bar{m}^{\alpha}_{H^+} \bar{c}^{\alpha}_{H^+}}{\kappa^{\alpha}} - \frac{\bar{m}^{\beta}_{OH^-} \bar{c}^{\beta}_{OH^-}}{\kappa^{\beta}} \right) \frac{i}{c^{\alpha}_{H^+} - \bar{c}^{\beta}_{OH^-}} \qquad (15)$$

Comparison of eqs 2 and 15 shows that the constituent concentration of H^+ in phase R, c_{jH^+R}, in the denominator of eq 2 becomes the concentration of H^+ c_{H^+R} in eq 15.

Computations of MCRB and Zwitterion Velocities. The MCRB systems used in this paper are boundaries 1 and 2, viz.,

boundary 1:
pH 2.85 formate buffer (+, R) jj[f] sodium formate +5.0 *í*g/mL Trp (-, *â*)
boundary 2:
pH 3.50 acetic buffer + 20 mM NaCl (+,R) jj[f] NaAc +1.0 *í*g/mL Trp (-, *â*)

In boundaries 1 and 2, the symbol of [f] indicates the boundary of jj moving toward the cathode. Boundary 1 is formed with the formic buffer and its conjugate salt. Boundary 1 is used for the stacking of Trp in phase *â* of sodium formate. Boundary 1 moves toward the cathode, and the running buffer is a mixture of formic acid and sodium formate; thus the velocities of boundary 1 should be computed with eq 15 as well as eq 16 given below, rather than eq 2 as has been proved in refs 33-35. The results of computations for boundary 1 are shown in Figure 2. The velocity of Trp in Ph 2.85 formate buffer is calculated with eqs 3 and 13; the computed velocities of Trp are also seen in Figure 2. Boundary 2 is created with acetic buffer and sodium acetate. Additionally, there is 20 mM NaCl in the acetic buffer. Thus, the boundary system is quite different from boundary 1. The boundary moves toward the cathode too, so its velocity should be evaluated

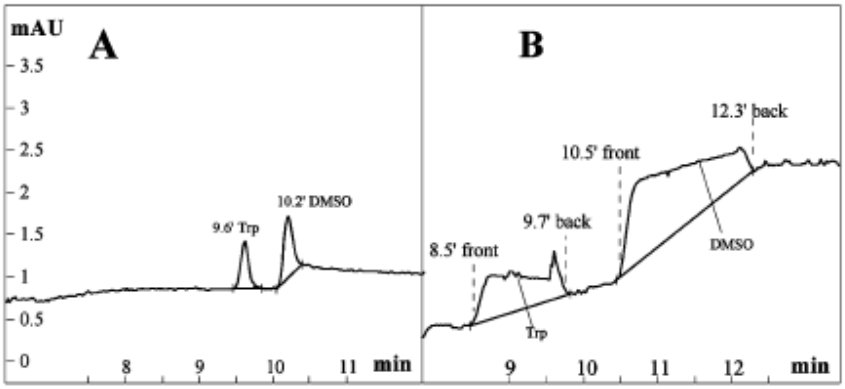

Figure 4. The normal electrophoregrams of CZE of Trp and DMSO in (A) 10- and (B) 120-s 15 mbar pressure injection sample plugs.Conditions: 40 mM pH 3.5 acetic running buffer, 1.0 *í*g/mL Trp and 0.03‰ DMSO dissolved in the running buffer, 50 cm total length (42 cm effective length), and 75-*í*m-i.d. capillary, 15 kV and 7-9 *í*A, detection at 214 nm, and 22 °C cooling air. The Trp and DMSO plateaus are observed in panel B; the vertical dotted lines indicate the times of the "front" and "back" ends of the two plateaus.

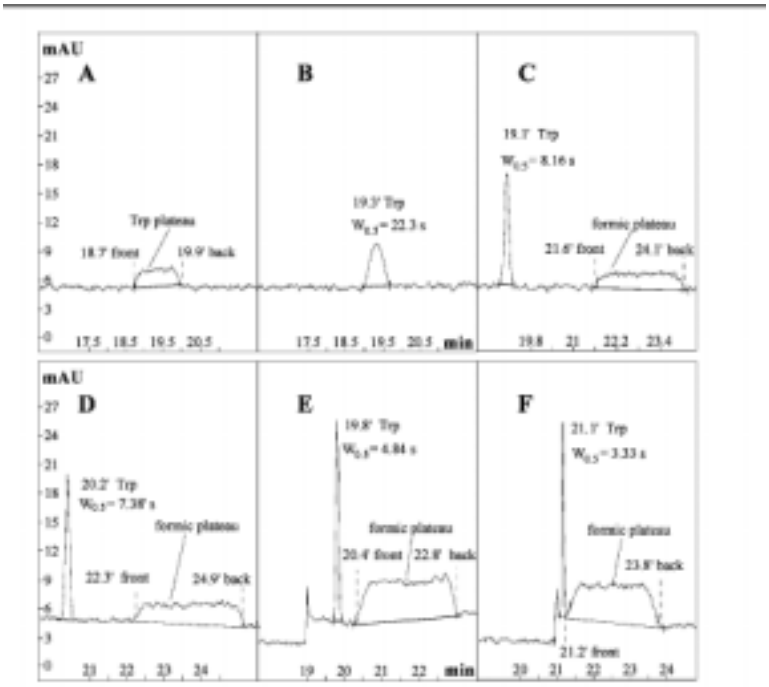

Figure 5. Stacking of 5.0 *í*g/mL Trp in 120-s 15 mbar pressure injection sample plug by the boundary system of 30 mM pH 2.85 formic buffer (+, R) jj (A) 20, (B) 40, (C) 60, (D) 80, (E) 100, or (F) 120 mM sodium formate (-, *â*). Conditions: capillary of total 65 and 50 cm effective lengths and i.d. 75 *í*m, 20 kV, and 21 *í*A, UV at 214 nm, and 22 °C air cooling. The formic plateau is observed in panels C-F rather than panels A and B; the formic plateau indicates the original sample plug neutralized mainly as formic acid. The vertical dotted lines indicate the times of "front" and "back" ends of formic plug (viz., original sample plug). The migration time and width ($W_{0.5}$) of Trp peak are also given in the individual panel (except for panel A in which only Trp plateau exists).

with eq 15 as well as eq 16 given below. The velocity of Trp in the running acetic buffer is also calculated by eqs 3 and 13. The curves of boundary 2 and Trp velocities are shown in Figure 3. The absolute mobilities of H^+ and OH^- at 25 °C, cited from ref 44, are respectively 36.3 _ 10^{-8} and 20.5 _ 10^{-8} m^2 V^{-1} s^{-1}. Before being used for the computation of boundary velocity with eq 15, the absolute mobilities should be corrected with the accurate equation developed from the previous empirical equations of ionic mobility[45-48]

$$m_{act} = m_0 \exp(-0.67(|z|)^{0.50}) \quad \text{(used for ion with } z = 1) \tag{16}$$

where m_{act} and m_0 are the actual and absolute mobilities,

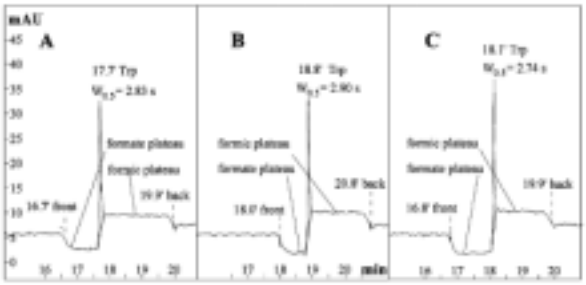

Figure 6. Stacking of 5.0 *í*g/mL Trp in 180-s 15 mbar pressure injection sample plug by the boundary system of 30 mM pH 2.85 formate buffer (+, R) jj (A) 80, (B) 100, and (C) 120 mM sodium formate (-, *â*). The other conditions are the same as those of Figure 5. The formic and formate plateaus are observed, the formic plateau indicates the original sample plug neutralized mainly as formic acid, and the formate plateau implies the unneutralized sodium formate in sample plug. The vertical dotted lines indicate the times of the "front" and "back" ends of whole sample plug injected. The migration time and width ($W_{0.5}$) of Trp peak are also given in the panels.

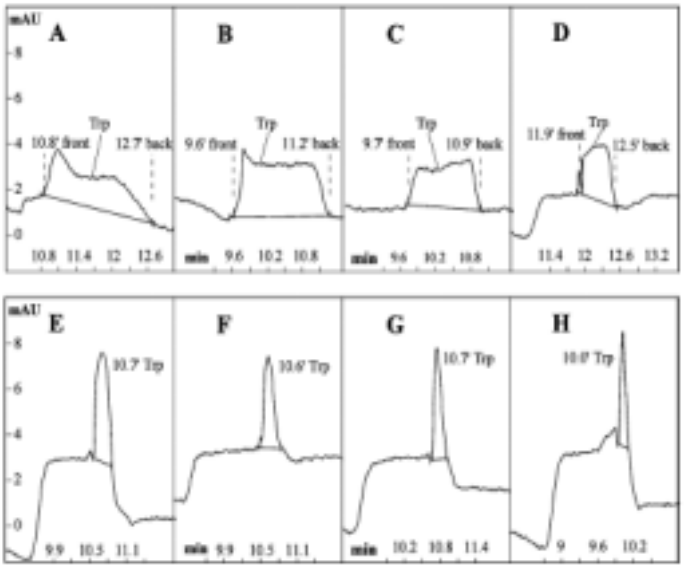

Figure 7. Stacking of 1.0 íg/mL Trp in 120-s 15 mbar pressure injection sample plugs by the boundary system of 40 mM pH 3.50 acetic buffer + 20 mM NaCl (+, R) jj (A) 10, (B) 20, (C) 30, (D) 40, (E) 50, (F) 60, (G) 70, and (H) 80 mM sodium acetate (-, â). The other conditions are the same as those of Figure 4.

respectively, *I* is the ionic strength, and *z* is the ionic valence. The ionic strength should be well controlled within 0.1 M, or eq 16 cannot well predict ionic mobility.

EXPERIMENTAL SECTION

Chemicals. Acetic acid (Analytical Reagent grade, AR),sodium acetate (AR), hydrochloric acid (AR), sodium chloride(AR), ammonia water (AR), dimethyl sulfoxide (DMSO, AR), formic acid (AR), sodium formate (AR), and L-tryptophan (Trp,Chrom pure) were purchased from the Shanghai Chemical Reagent Co. (Shanghai, China). Sodium hydroxide (GuaranteedReagent grade, GR) was from the Shanghai Zhuangong Reagent Factory (Shanghai, China). The basic physical chemical paratmeters of Trp, which will be used for the calculation of mobility, are given in Table 1.

Apparatus. A high-performance capillary electrophoresis (HPCE) apparatus (ACS 2000, Beijing Cailu Instrumental Co., Beijing, China) was used. The HPCE was equipped with a power supply (up to constant voltage 30 kV), a HW-2000 chromatography workstation, and a UV-visible detector (duoble light beams, ì) 190-720 nm, set at 214 nm). Two fused-silica capillaries were used (the Factory of Yongnian Optical Fiber, Hebei, China). One is a tube with total length 50 cm, effective length 42 cm, and i.d. 75 ím, and another with total 60 cm, effective 45 cm and i.d. 75 ím.The runs were carried out under 22 °C cooling air. Before each run, the new capillaries were conditioned by rinsing with 1.0 M NaOH for 20 min, ultrapure water for 10 min, 1.0 M HCl for 20 min, and running buffer for 30 min, in order. A pure water system (SG Wasseraufbereitung und Regenerierstation Gmbh) was used to produce the ultrapure water with the specific conductivity down to 0.055 íS/cm. If necessary, a conductance meter was used for the detection of specific conductivity of the running buffer or sample matrix at 25 °C, due to some key important data like the absolute mobilities of H^+ and OH^-, which are used to compute the boundary velocity, are obtained at 25 °C

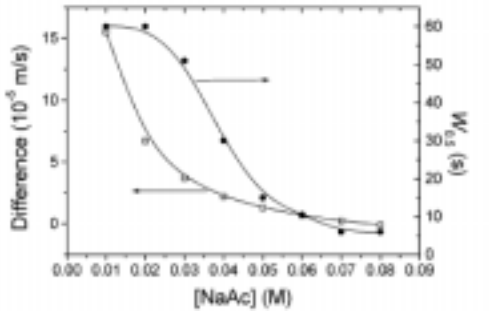

Figure 8. Relations between velocity difference () $V_{Rá} - V_{Trp\ R}$)
and Trp peak width ($W_{0.5}$) at half-height as a function of the concentration of sodium acetate in the sample matrix (viz., phase â) in Figure 7. The conditions are the same as these in Figure 7.

Table 2. Content, Ionic Strength, and Conductivity of Weak Alkaline Sample Matrix Prepared with Sodium Formate.

no.	Trp (μg/mL)	sodium formate (mM)	ion strength (mM)	κ (S/m)[a]
1	5.0	20	20	0.192
2	5.0	40	40	0.370
3	5.0	60	60	0.529
4	5.0	80	80	0.702
5	5.0	100	100	0.860
6	5.0	120	120	1.042

[a] Conductivity at 25 °C.

Buffer and Sample Matrix. Two kinds of running buffers were used. The first was pH 2.85 30 mM formic buffer (ionic strength *I*) 0.0033 M, _) 0.078 S/m at 25 °C). The second was pH 3.50 40 mM acetic buffer + 20 mM NaCl (*I*) 0.0212 M, _) 0.256 S/m at 25 °C). Three kinds of sample matrixes were prepared. The first kind was the normal sample matrix prepared with the pH 3.50 40 mM acetic buffer (1.0 *í*g/mL Trp and 0.03‰ DMSO). The second was the weak alkaline sample matrix made with sodium formate in Table 2. And the third was the one made with sodium acetate (see Table 3). Before being used, the buffers and samples were degassed and centrifuged at 5000 rpm for 10 min, if necessary.

General Stacking of MCRB. First, the anodic end of the capillary was inserted into an alkaline salt sample, and then 15 mbar pressure was used for sample injection. Second, the sample vial was displaced with the anodic vial containing the running buffer as shown in Figure 1A. Third, the power supply was turned on and a MCRB was created between the running buffer (holding H^+) in the anodic vial and the alkaline sample (holding OH^-) as shown in Figure 1A and B. The MCRB was used for the stacking of zwitterion in CE. During the experiments, the high-voltage power supply should be operated with extreme care to avoid electric shock. In addition, one ought to avoid the harmful action of sodium hydroxide and hydrochloric acid to one's eyes and skin.

Table 3. Content, Ionic Strength, and Conductivity of Alkaline Sample Matrix Prepared with Sodium Acetate

no.	Trp (μg/mL)	sodium acetate (mM)	ion strength (mM)	κ (S/m)[a]
1	1.0	10	10	0.085
2	1.0	20	20	0.166
3	1.0	30	30	0.244
4	1.0	40	40	0.319
5	1.0	50	50	0.393
6	1.0	60	60	0.465
7	1.0	70	70	0.536
8	1.0	80	80	0.605

[a] Conductivity at 25 °C.

RESULTS AND DISCUSSIONS

Normal Capillary Zone Electrophoresis (CZE) and Mobility of Trp. Figure 4 shows the normal CZE of Trp and DMSO, viz., the EOF marker. In Figure 4A and 4B, the injection times are respectively 10 and 120 s. The comparisons between parts A and B of Figure 4 evidently show that the peaks of Trp and DMSO become much wider when the injection time is increased to 120 s. From the data of Figure 4A, the mobility of Trp is detected; the detected constituent mobility of Trp in pH 3.50 40 mM acetic buffer is 0.13 _ 10^{-8} m^2 V^{-1} s^{-1}. With the effective mobility of Trp, as well as other data in Table 1, one can calculate the mobility of positive monovalent charged Trp, as shown in Table 1.

Stacking Conditions of Trp in Formic System. Figure 2 shows the MCRB and Trp velocities in boundary 1 and the"crossover point" of two velocity curves very near 60 mM sodium formate. The crossover is a key point. Over the crossover point, the velocity of the boundary is greater than that of Trp if less than 60 mM sodium formate is used; conversely, under the point, the velocity of the boundary is less than that of Trp if greater than 60 mM sodium formate is used. Thus, in accordance with expressions 12 and 14, Figure 2 reveals the following four theoretical predictions. (1) If 20 mM sodium formate is used to form the MCRB, the velocity of the boundary is highly faster than that of Trp; hence, bad stacking of the Trp sample plug exists.

(2) If 40 mM sodium formate is used, the velocity of the boundary decreases obviously, but still is much higher than that of Trp, so fair stacking of Trp ought to be realized. (3) If 60 mM sodium formate is used, the velocity of MCRB is slightly less than that of Trp; thus, an excellent stacking must be achieved. (4) If greater than 60 mM sodium formate is used, the velocity of the boundary is much less than that of Trp; theoretically the boundary gives its same good stacking to a Trp analyte. The four predictions from Figure 2 are well demonstrated by the following experiments in Figures 5 and 6. Figure 5A shows the presence of a wide Trp plateau is present when 20 mM sodium formate is used to prepare

the sample matrix. Similar results are further shown in Figure S1 (Supporting Information) in which wider and wider Trp plateaus exist if the time of sample injection increases from 60, to 180, and 300 s. The results in Figure 5A and Figure S1 strong verify the first prediction above. Figure 5B, as well as Figure S2, exhibits the fair stacking of Trp under the conditions of 40 mM sodium formate used as the sample buffer; the comparisons between Figures S1 and S2 further prove the partial stacking occurring in Figure 5B. Clearly, the experimental results concur with the second prediction above; Figure 5C highlights the good stacking of Trp when 60 mM sodium formate is used to prepare the matrix. The experiments are in agreement with the third theoretical prediction above.

Table 4. Comparisons between the Stackings Induced by the Anodic Direction Electromigration of Trp in Phase *β* and by the MCRB in Figure 5C−F

	in phase α	in phase β (sodium formate)			
	formic buffer	Figure 5C	Figure 5D	Figure 5E	Figure 5F
concentration (mM)	30	60	80	100	120
pH value	2.85	8.27	8.33	8.38	8.42
κ (S m^{-1})	0.075	0.539	0.702	0.860	1.012
E (V m^{-1})[a]	2.90×10^4	0.42×10^4	0.32×10^4	0.26×10^4	0.22×10^4
μ_{ep} (m^2 s^{-1} V^{-1})[b]	0.84×10^{-4}	-0.22×10^{-4}	-0.24×10^{-4}	-0.27×10^{-4}	-0.29×10^{-4}
V_{EOF} (m s^{-1})		2.34×10^{-4}	1.77×10^{-4}	1.42×10^{-4}	1.19×10^{-4}
V_{Trp}^{β} or V_{Trp}^{β}/(m s^{-1})[a]	2.45×10^{-4}	-0.20×10^{-4}	-7.74×10^{-5}	-7.11×10^{-5}	-6.49×10^{-5}
$V_{Trp}^{\alpha}/V_{EOF}^{\alpha}$ or $V_{Trp}^{\beta}/V_{EOF}^{\beta}$	>100%	3.93%	4.37%	5.00%	5.45%

[a] The current intensity is set at 2265 A m^{-2} (set in accordance with the runs in Figure 5; see Figure 2). [b] The negative sign of before the data indicates the Trp in phase *β* migrating toward the anode.

These results of Figures 5D-F and 6 as well as Figures S3 and S4 manifest the validity of the fourth prediction of the good stacking if greater than 60 mM sodium formate is used as the sample buffer. In Figure 5D (80 mM sodium formate is used as the buffer of matrix), the stacked peak of Trp (the peak width at half-height $W_{0.5}$) 7.38 s) becomes slightly thinner than that ($W_{0.5}$) 8.15 s) in Figure 5C. In Figure 5E (100 mM sodium formate), the value of $W_{0.5}$ is decreased to 4.84 s. In Figure 5F (120 mM sodium formate), the $W_{0.5}$ is reduced to 3.33 s. If the time of sample injection is increased to 180 s, Parts D-F of Figure 5 are respectively exchanged as Figure 6A-C, in which the values of $W_{0.5}$ are only from 2.74 to 2.90 s, being sharp and quite constant. These results indicate the same tight stacking to the Trp sample plug if 80, or 100, or 120 mM sodium formate is used. If the injection time is further increased, as shown in Figure S3 (including Figure S4), the values of $W_{0.5}$ are _2.50 s, being slight less than these in Figure 6. The slight decrease of $W_{0.5}$ in Figure S3 and S4 is caused because the migration time of Trp peak becomes short due to the faster electroosmotic flow (EOF) induced by more alkaline sample injected. Evidently, Figures 5D-F and 6 as well as Figures S3 and S4 well prove the same tight stacking to Trp plugs, if g60 mM sodium formate is used to prepare the sample matrix. This concurs with the fourth prediction, as well as the third one. Whereas, if 20 or 40 mM sodium formate is used, no such tight stacking occurs as shown in Figures S1 and S2.

The tightly stacked Trp peaks exist in the progressing MCRB that ends after the detector as shown in Figures 6, S3, and S4, rather than the MCRB that ends before the detector as displayed in Figure 5. If a larger volume sample is injected (see Figure 6), the time of complete reaction between phases R and *â* becomes longer than that with less sample injection (see Figure 5D-F). Hence, the boundaries in Figures 6, S3, and S4 are still in their progress, when they pass through the detector (due to the EOF migrating toward the cathode). In Figures 6,S3, and S4, the formic plateau with high absorbance indicates the stacked Trp sample plug, which is mainly neutralized as formic acid by the H_+ electromigrating from phase R into the boundary; the formate plateau with low absorbance implies the sodium formate in the unstacked sample plug that is still unneutralized by the H_+, when passing through the detector. The whole length of original sample injection is that from the “front” time to the “back”, and the tightly stacked peak of Trp indicates position (or time) of the MCRB that is just passing through the detector. Consequently, the tightly MCRB-stacked Trp peak goes through the detector without the evident diffusion of Trp peak, which always occurs after the end of MCRB before the detector (see Figure 5C-F). Therefore, under the condition of large-volume sample injection as well as the existence of $V_{Rá}$ e$V_{Z\,R}$, we can observe the same tightly MCRBstacked peaks of Trp existing in Figures 6, S3, and S4, rather than Figure 5C-F.

The enhancement of Trp stacking shown in Figure 5C-F is induced by the gradually shortened time of diffusion of tightly MCRB-stacked peak of Trp after ends of MCRB. From Figure 5C-F, the widths of formic plateaus are respectively 2.5, 2.6, 2.4, and 2.6 min; this means the volumes of actual sample injection are almost equal to each other. Under the condition of same sample volume, the complete neutralization of higher concentration sodium formate in the sample plug needs a higher quantity of H_+ electromigrating from phase R into the boundary, viz., more electroneutralization time of H_+. The length from the anode end of capillary to the detector is constant. Hence, the more electroneutralization time leads to less separation time of the tightly stacked Trp peak and further results in less diffusion time of the tightly MCRB-stacked Trp peak, if more concentration of sodium formate is used. The less diffusion time gradually induces the sharper Trp peaks observed in Figure 5C-F, in which the width (viz., diffusion

time) between the stacked peak and the front of the formic plateau becomes shorter and shorter. The anodic direction electromigration of negatively charged Trp in phase *â* has a contribution to the Trp stacking. The contribution is computed and compared with that of MCRBinduced stacking as given in Table 4. The ratio of $V_{Trp\,â}/V_{Râ}$ is generally less than 5%, which indicates the weak stacking efficiency of the anodic direction electromigration of Trp in phase *â*. The weak stacking is induced for the following reasons (see Table 4): (1) the much lower electric field in phase *â* in contrast to the higher in phase R; (2) the slow mobility of Trp in phase *â* in contrast to the fast in phase R. Owing to the weak stacking as compared with the MCRB-induced stacking, it is found that the tightly stacked peak height should be in proportion to the length of the formic plateau, viz., the width of actually stacked sample plug. The analysis is well proved by the results in Figure S5.

Stacking Conditions of Trp in Acetic System. To further test the validity of the theoretical procedure developed in this paper, boundary 2 is used for the fine investigations on MCRBinduced stacking of Trp. Figure 3 shows the theoretical computations of velocities of Trp and boundary 2 and the crossover point of the velocity curves very near 70 mM sodium acetate. From the computations in Figure 3, the four theoretical conclusions are drawn below. (1) If 10-30 mM sodium acetate is used as the sample matrix, viz., phase *â*, the boundary velocity is much faster than the Trp velocity; hence, the MCRB cannot stack the Trp plug, the stacking of Trp plug is poor. (2) If 40-50 mM sodium acetate is used to prepare the sample matrix, the boundary velocity decreases greatly and is near the Trp velocity; hence, the obvious stacking should be present. (3) If 60 mM sodium acetate is used, the boundary velocity is much near that of Trp; theoretically quite good stacking to the Trp plug is induced. (4) If 70 mM or more concentration sodium acetate is used, the boundary velocity is equal to or less than that of Trp, so excellent stacking of Trp plug should be achieved. These fine theoretical results are well manifested by the following experiments.

Figure 7 shows the stacking results of Trp by boundary 2. Parts A-C of Figure 7 show that the peaks of Trp are quite wide, being similar to that of Trp in Figure 5A; the result implies the weakly MCRB-induced stacking to Trp in the sample matrix; this is in agreement with the first prediction of Figure 3. Parts D and E of Figure 7 show that the peaks of Trp become thinner than these in Figure 7A-C, but still wider than those in Figure 7F-H. The results indicate the obvious but still partial stacking to Trp plug. The results are in good coincidence with the second prediction of Figure 3. Evidently, Figure 7F shows a quite good Trp peak stacked by the boundary formed with 60 mM sodium acetate and the acetic buffer; this result verifies the third prediction of Figure 3. The Trp peaks in Figure 7G and H, which is evidently thinner than that of Figure 7F, are equal to 6.0 s (being equal to each other). The results in Figure 7G and H prove the fourth theoretical conclusion. Figure 8 further shows the good relation between the peak width of Trp and the difference of boundary and Trp velocities. The fine comparisons of peak widths in Figure 8 show that the stacking to Trp plug becomes the good (Figure 7G and H) from the bad (A-C), to the obvious (D and E), to the quite good (F). This is in good agreement with the whole trend predicted by Figure 3 and expressions 12 and 14.

General Conditions of Stacking Zwitterion by MCRB. The choices of pH values of phases R and *â* should be designed in accordance with the requirement of inequalities 6 and 7 (or inequality 8 if possible), or you cannot stack a zwitterionic analyte completely. This principle was used in ref 29 and this paper. For example, in the experiments of stacking Trp in Figure 5, the p*I* of Trp equals 5.48; the pH values of the acidic running and alkaline sample buffers are respectively 2.85 and 8.45, which comprise the p*I* of Trp () 5.48).

Stacking Type of Zwitterion and Its Applications. There are at least four basic types of MCRB-induced stacking of zwitterion (see Figure S6): (1) cathodic direction boundary and analyte in phase *â*, (2) anodic direction boundary and analyte in phase *â*, (3) cathodic direction boundary and analyte in phase R, and (4) anodic direction boundary and analyte in phase R. This paper concerns the first type of stacking of zwitterion. The first type is of powerful efficacy. The work[30] shows that (1) the results achieved in this paper can be directly used in the powerful stacking of zwitterion in the whole capillary sample plug and (2) greater than 3-million-fold enhancement of detection sensitivity of zwitterion in CE can be easily achieved by using a single MCRBinduced stacking. The second type has been used for the selective high-efficiency stacking of oxytocin and at least 20 millionfold stacking has been easily achieved (we can support the unpublished data, if necessary).

CONCLUSIONS

From the above results and discussion, one can reach the following conclusions. (1) The running buffer and sample matrix should be designed carefully in accordance with expressions 6-9. (2) To efficiently stack zwitterionic analytes, MCRB velocity in the mode used in this paper (see Figure 1A) should be designed from zero to the velocity of the zwitterion in the acidic running buffer, or the MCRB can only partially (even poorly) stack zwitterionic analytes. (3) The two theoretical results are well proved by the relative experiments. (4) Thus, the MCRB theory can be well used to predict accurate stacking conditions of the zwitterion and the stacking efficiency of the zwitterion under different stacking conditions. In addition, the experiments also show the tightly stacked peak of the zwitterion existing in the process of MCRB, but not after the MCRB before the detector.

ACKNOWLEDGMENT

The authors are grateful for funding provided by the NSFC (29775014, 20245004, and 20475036) and the Committee

of Science and Technology of Anhui Province (01043905).

SUPPORTING INFORMATION AVAILABLE

Additional information as noted in text. This material is available free of charge via the Internet at http://pubs.acs.org.

Received for review April 6, 2004. Accepted September 1, 2004.
AC049470S

(1) Boc˘ek, P.; Deml, M.; Gebauer, P.; Dolnik, V. In *Analytical Isotachophoresis; Electrophoresis Library*; Radola, B. J., Ed.; VCH: Weiinheim, Germany, 1988; pp 1-9, 43-47.
(2) Gebauer, P.; Thormann, W.; Boc˘ek, P. *J. Chromatogr.* **1992**, *608*, 47-57.
(3) Jandik, P.; Jones, W. R. *J. Chromatogr.* **1991**, *546*, 431-443.
(4) Chien, R. L.; Burgi, D. S. *J. Chromatogr.* **1991**, *559*, 141-152.
(5) Chien, R. L.; Helmer, J. C. *Anal. Chem.* **1991**, *63*, 1354-1361.
(6) Chien, R. L.; Burgi, D. S. *Anal. Chem.* **1991**, *63*, 2042-2047.
(7) Chien, R. L.; Burgi, D. S. *Anal. Chem.* **1992**, *64*, 489A-496A.
(8) Chien, R. L.; Burgi, D. S. *Anal. Chem.* **1992**, *64*, 1046-1050.
(9) Quirino, J. P.; Terabe, S. *Science* **1998**, *282*, 465-468.
(10) Yang, L.; He, Y. Z.; Gan, W. E.; Lin, X. Q. *J. Chromatogr., A* **2001**, *932*, 13-20.
(11) Zhang, Y. K.; Zhu, J.; Zhang, L. H.; Zhang, W. B. *Anal. Chem.* **2000**, *72*, 5744-5747.
(12) Quirino, J. P.; Terabe, S. *Anal. Chem.* **2000**, *72*, 1023-1030.
(13) Quirino, J. P.; Terabe, S. *Electrophoresis* **2000**, *21*, 355-359.
(14) Quirino, J. P.; Terabe, S.; Boc˘ek, P. *Anal. Chem.* **2000**, *72*, 1934-1940.
(15) Quirino, J. P.; Kim, J. B.; Terabe, S. *J. Chromatogr.; A* **2002**, *965*, 357-373.
(16) Palmer, J.; Munro, N. J.; Landers, J. P. *Anal. Chem.* **1999**, *71*, 1679-1687.
(17) Palmer, J.; Burgi, D. S.; Munro, N. J.; Landers, J. P. *Anal. Chem.* **2001**, *73*,725-731.
(18) Palmer, J.; Burgi, D. S.; Landers, J. P. *Anal. Chem.* **2002**, *74*, 632-638.
(19) Britz-McKibbin, P.; Chen, D. D. Y. *Anal. Chem.* **2000**, *72*, 1242-1252.
(20) Britz-McKibbin, P.; Bebault, G. M.; Chen, D. D. Y. *Anal. Chem.* **2000**, *72*,1729-1735.
(21) Britz-McKibbin, P.; Ichihashi, T.; Tsubota, K.; Chen, D. D. Y.; Terabe, S. *J. Chromatogr., A* **2003**, *1013*, 65-76.
(22) Hadwiger, M. E.; Torchia, S. R.; Park, S. R.; Biggin, M. E.; Lunte, C. E. *J. Chromatogr., B* **1996**, *681*, 241-249.
(23) Zhao, Y. P.; Lunte, C. E. *Anal. Chem.* **1999**, *71*, 3985-3991.
(24) Ward, E. M.; Smyth, M. R.; O'Kennedy, R.; Lunte, C. E. *J. Pharm. Biomed.* **2003**, *32*, 813-822.
(25) Arnett, S. D.; Lunte, C. E. *Electrophoresis* **2003**, *24*, 1745-1752.
(26) Shihabi, Z. K. *Electrophoresis* **2002**, *23*, 1612-1617.
(27) Shihabi, Z. K. *Electrophoresis* **2002**, *23*, 1628-1632.
(28) Cao, C. X.; He, Y. Z.; Li, M.; Qian, Y. T.; Yang, L.; Qu, Q. S.; Zhou, S. L.; Chen, W. K. *J. Chromatogr., A* **2002**, *952*, 39-46.
(29) Cao, C.-X.; He, Y.-Z.; Li, M.; Qian, Y.-T.; Gao, M.-F.; Ge, L.-H.; Zhow, S.-L.; Yang, L.; Qu, Q.-S. *Anal. Chem.* **2002**, *74*, 4167-4174.
(30) Cao, C. X.; Qin, W. H.; Liu, W.; Li, S.; Zhang, W. *Anal. Chem.*, submitted. Cao, C. X.; Qin, W. H.; Li, S.; Zhang, W. *J. Am. Chem. Soc.*, in revision.
(31) Cao, C. X. *Acta Chem. Scand.* **1998**, *52*, 709-713.
(32) Cao, C. X. *J. Chromatogr., A* **1998**, *813*, 153-171.
(33) Cao, C. X.; Zhou, S. L.; He, Y. Z.; Qian, Y. T.; Yang, L.; Qu, Q. S.; Gan, W. E.; Dong, L.; Zhou, Y. Q.; Chen, W. K. *J. Chromatogr., A* **2001**, *907*, 347-352.
(34) Cao, C. X.; Zhou, S. L.; Qian, Y. T.; He, Y. Z.; Yang, L.; Qu, Q. S.; Chen, W. K. *J. Chromatogr., A* **2001**, *922*, 283-292.
(35) Zhou, S. L.; Cao, C. X.; Qian, Y. T.; He, Y. Z.; Yang, L.; Qu, Q. S.; Chen, W. K. *Prog. Nat. Sci.* **2002**, *12*, 667-672.
(36) MacInnes, D. A.; Longsworth, L. G. *Chem. Rev.* **1932**, *11*, 171-230.
(37) Dole V. P. *J. Am. Chem. Soc.* **1945**, *67*, 1119-1126.
(38) Svensson, H. *Acta Chem. Scand.* **1948**, *2*, 841-855.
(39) Alberty, R. A. *J. Am. Chem. Soc.* **1950**, *72*, 2361-2367.
(40) Nichol, J. C. *J. Am. Chem. Soc.* **1950**, *72*, 2367-2375.
(41) Mckee, T.; Mckee, J. R. *Biochemistry*; Wm. C. Brown Publishers: Dubuque, IA, 2002; pp 77-84.
(42) Svensson, H. *Acta Chem. Scand.* **1961**, *15*, 325-341.
(43) Svensson, H. *Acta Chem. Scand.* **1962**, *16*, 456-466.
(44) David, R. L. *CRC Handbook of Chemistry and Physics*, 73rd ed.; CRC Press:Boca Raton, FL, 1992-93; p D-167.
(45) Reijenga, J. C.; Kenndler, E. *J. Chromatogr., A* **1994**, *659*, 403-415.
(46) Friedl, W.; Reijenga, J. C.; Kenndler, E. *J. Chromatagr., A* **1995**, *709*, 163-170.
(47) Cao, C. X. *J. Chromatogr., A* **1997**, *771*, 374-348.
(48) Cao, C. X. *J. High Resolut. Chromatogr.* **1997**, *20*, 701-702.